

# Dielectric spectroscopy for bioanalysis: From 40 Hz to 26.5 GHz in a microfabricated wave guide

G. R. Facer<sup>a)</sup>

*Department of Physics, Princeton University, Princeton, New Jersey 08544*

D. A. Notterman

*Department of Molecular Biology, Princeton University, Princeton, New Jersey 08544*

L. L. Sohn

*Department of Physics, Princeton University, Princeton, New Jersey 08544*

(Received 21 September 2000; accepted for publication 18 December 2000)

We report developing coplanar waveguide devices which can perform dielectric spectroscopy on biological samples within a microfluidic channel or well. Since coupling to the fluid sample is capacitive, no surface functionalization or chemical sample preparation are required. Data on cell suspensions and solutions of proteins and nucleic acids spanning the frequency range from 40 Hz to 26.5 GHz are presented. Low-frequency data are well explained using a simple dispersion model. At microwave frequencies, the devices yield reproducible and distinguishable spectral responses for hemoglobin solution and live *E. coli*. © 2001 American Institute of Physics.  
[DOI: 10.1063/1.1347020]

Rapid characterization of biological specimens is increasingly important in research and clinical applications. While current optical and chemical detection techniques<sup>1–3</sup> can effectively analyze biological systems, a number of disadvantages restrict their versatility. As examples: most samples must be chemically altered prior to analysis, and photobleaching can place a time limit on optically probing fluorophore-tagged samples. Purely electronic techniques provide solutions to many such problems, as they can probe a sample and its chemical environment directly over a range of time scales, without requiring chemical modifications.<sup>4,5</sup> One example of electronic detection is dielectric spectroscopy:<sup>6–10</sup> examining permittivity as a function of frequency. This direct, nondestructive, and sensitive technique can probe a system at various length scales, from centimeters to microns, with sample volumes as small as picoliters.<sup>11,12</sup>

In this letter, we describe coplanar waveguide (CPW) devices for performing dielectric spectroscopy on samples confined to a microfluidic channel or well across nearly 9 orders of magnitude in frequency, from 40 Hz to 26.5 GHz. Because coupling to the sample is capacitive, our CPWs allow measurements from dc to microwave frequencies, *without* the need for surface functionalization or chemical binding.<sup>12</sup> A very wide range of species can therefore be analyzed rapidly and directly. The planar geometry of our devices allows for straightforward integration with microfluidic systems.<sup>5,13,14</sup> Below, we discuss the fabrication of the CPW devices, and the low-frequency to microwave spectra which we have obtained for biomolecular solutions and cell suspensions.

Permittivity measurements across a range of frequencies (“dielectric spectra”) provide information about the species present and their chemical environment. Features in dielectric spectra—all relating to polarization relaxations<sup>7,15–18</sup>—

are generally classified as  $\alpha$ -,  $\beta$ -, or  $\gamma$ -dispersions.  $\alpha$ -dispersion is the permittivity enhancement by rearrangements of small ions, including screening at the fluid interface.  $\beta$ -dispersion arises from distortions of cellular membranes and macromolecules.  $\gamma$ -dispersion is due to rotations and deformations of small, polar molecules or groups (frequently the solvent itself). Access to a broad frequency range is imperative with biological samples, due to their chemical diversity:<sup>19,20</sup> in solutions with total ionic strengths  $\geq 0.1$  M,  $\alpha$ -dispersion extends up to  $\geq 1$  GHz, while  $\beta$ -dispersions extend from  $\leq 1$  kHz<sup>21</sup> up to the relaxational modes of macromolecules in the infrared (THz) and beyond.

Dielectric spectra for  $\alpha$ -,  $\beta$ -, and  $\gamma$ -dispersions have a common form:<sup>15,22</sup> at low frequencies, the polarization is able to closely follow the applied electric field (relative permittivity  $\epsilon = \epsilon_{LF}$ ), while at high frequencies applied excitations oscillate too fast for the charges to respond ( $\epsilon = \epsilon_{HF}$ ). Generally,  $\epsilon_{LF} \gg \epsilon_{HF}$ .

A schematic diagram of our CPW devices is shown in Fig. 1. They are symmetric metal transmission lines comprised of a 40  $\mu\text{m}$  wide central strip bordered by two grounded 380  $\mu\text{m}$  wide conductors. Each metal region is an evaporated Ti/Au (50 Å/500 Å) base topped with an elec-

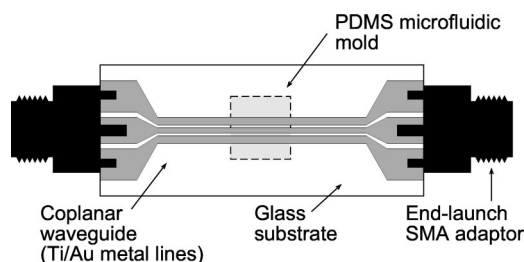


FIG. 1. CPW device, showing the Ti/Au wave guide (not to scale) and microfluidic sample containment. Across the central portion, the inner line width is 40  $\mu\text{m}$ , outer line widths 380  $\mu\text{m}$ , and the inner–outer separation is 7  $\mu\text{m}$ . Total substrate length is 34 mm.

<sup>a)</sup>Electronic mail: gfacer@princeton.edu

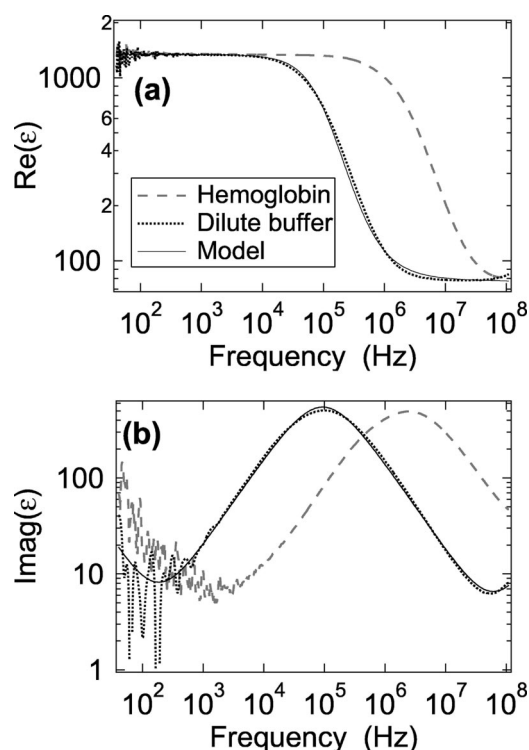


FIG. 2. Relative permittivity data: real (a) and imaginary (b) components. Solid traces are from hemoglobin (100  $\mu\text{g/mL}$ ), dashed traces for Tris buffer (1 mM, pH 8), and dotted curves are Cole-Cole calculations as per Eq. (1) (parameters  $\epsilon_{\text{LF}} - \epsilon_{\text{HF}} = 1340$ ,  $\tau = 1.70 \mu\text{s}$ ,  $\alpha = 0.91$ , and  $\sigma_{\text{LF}} = 40 \text{ nS}$ ).

trodeposited gold layer (total Au thickness 1  $\mu\text{m}$ ). The substrate is glass, and connection is via end-launch subminiature (SMA) adaptors. Capacitive coupling to the fluid is achieved by encapsulating the metal lines in 1000  $\text{\AA}$  of plasma enhanced chemical vapor deposition-grown silicon nitride. Silicone [poly(dimethylsiloxane)] confines the fluid.

At frequencies below  $\sim 100 \text{ MHz}$ , the relative permittivity is obtained from the impedance  $Z$  via  $\epsilon = 1/j\omega ZC_0$  ( $C_0$  is the capacitance through the sample volume when empty, typically  $\sim 10 \text{ fF}$ ).  $Z$  data are obtained with a Hewlett-Packard 4294A impedance analyzer (excitation amplitude 500 mV). We have confirmed that the data are free of non-linear conductive effects. Microwave data ( $\geq 45 \text{ MHz}$ ) are phase-sensitive transmission and reflection coefficients ("S parameters") at the adaptors, obtained with a Hewlett-Packard 8510C vector network analyzer.

We have examined a variety of samples, including solutions of hemoglobin (derived from washed and lysed human red blood cells) and bacteriophage  $\lambda$ -deoxyribonucleic acid (DNA), and live *E. coli* suspensions. The concentration of hemoglobin is 100  $\mu\text{g/mL}$  in 0.25 M Tris buffer (pH 8), and that of DNA is 500  $\mu\text{g/mL}$ , in 10 mM Tris and 1 mM EDTA (pH 8) buffer. *E. coli* are suspended in 85% 0.1 M  $\text{CaCl}_2/15\%$  glycerol. For the measurements, we have employed both molded microfluidic channels and simpler enclosed wells. Results are consistent (within a scaling factor for the fluid-CPW overlap length) for sample volumes ranging from  $\leq 3 \text{ pL}$  to  $\geq 20 \mu\text{L}$ . For the following discussions, we present data from capped 10  $\mu\text{L}$  wells.

Figure 2 shows  $\epsilon$  from 40 Hz to 110 MHz, for hemoglobin, dilute Tris buffer (concentration 1 mM, pH 8), and a

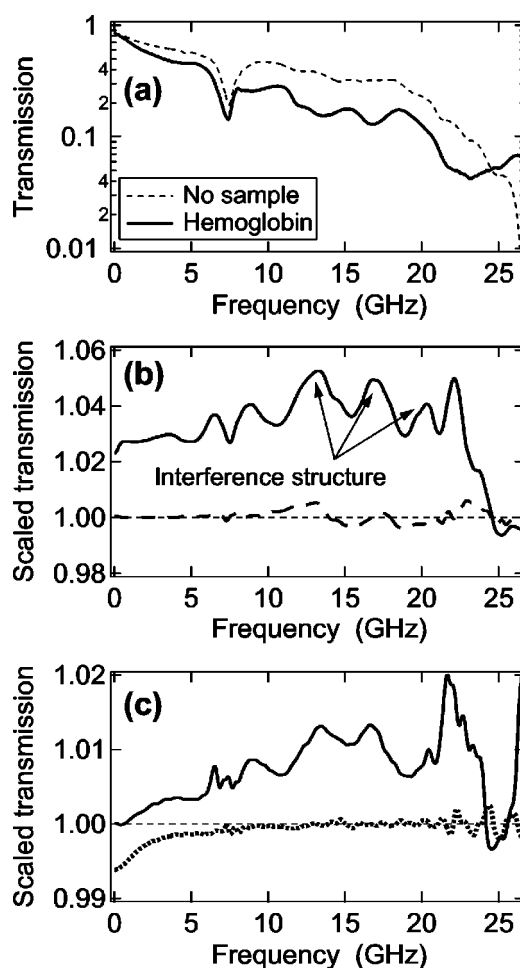


FIG. 3. Microwave transmission data. (a) Raw data, for the cases of no sample (dotted) and a 100  $\mu\text{g/mL}$  hemoglobin solution (solid). (b) Normalized data (using the respective buffers) for 100  $\mu\text{g/mL}$  hemoglobin (solid trace) and 500  $\mu\text{g/mL}$  phage  $\lambda$ -DNA (dashed), showing the difference in their microwave responses. (c) Solid trace is the (buffer-normalized) response of *E. coli*, and the dotted trace is that of the Tris buffer from the hemoglobin solution (normalized using deionized  $\text{H}_2\text{O}$ ).

Cole-Cole<sup>7</sup> model calculation relating  $\epsilon$  to the angular frequency  $\omega$

$$\epsilon = \epsilon_{\text{HF}} + \frac{\epsilon_{\text{LF}} - \epsilon_{\text{HF}}}{1 + (j\omega\tau)^\alpha} - j \frac{\sigma_{\text{LF}}}{\omega}. \quad (1)$$

Here  $\epsilon_{\text{LF}} - \epsilon_{\text{HF}}$  is the "dielectric increment,"  $\tau$  is a characteristic time constant,  $\alpha \leq 1$  defines the sharpness of the transition, and  $\sigma_{\text{LF}}$  is the dc conductivity. For the calculation in Fig. 2,  $\epsilon_{\text{LF}} - \epsilon_{\text{HF}} = 1340$ ,  $\tau = 1.70 \mu\text{s}$ ,  $\alpha = 0.91$ , and  $\sigma_{\text{LF}} = 40 \text{ nS}$ . A small series resistance (90  $\Omega$ ) is included in the model to fit high-frequency loss within the CPW.

The spectra in Fig. 2 show two features. First, the dielectric increment of the high-frequency transition is a constant of the measurement geometry. Second, and in contrast, the  $\epsilon_{\text{LF}} \rightarrow \epsilon_{\text{HF}}$  transition frequency is directly proportional to the total ionic strength of the solution. As shown, the dispersion model [Eq. (1)] describes the data very well.

Figure 3 shows transmission data from 45 MHz to 26.5 GHz. In Fig. 3(a), raw transmission and reflection are shown for two control cases: a dry sample setup, and deionized water. Figures 3(b) and 3(c) contain transmission data sets for hemoglobin, DNA, and live *E. coli* which have been normalized with respect to their corresponding buffers. Fig-

ure 3(c) also shows (dotted trace) transmission data from the buffer used for hemoglobin measurements, normalized using deionized water data. This, in particular, demonstrates that even at high salt concentrations (0.25 M Tris-HCl) the microwave effects of buffer salts are limited to a monotonic decrease in transmission below 10 GHz.

Three descriptive notes should be made regarding the data: first, periodic peak and trough features [such as those marked by arrows in Fig. 3(b)] are interference effects due to reflections at the SMA adaptors and the fluid itself. Second, the SMA adaptors impose the high-frequency cutoff at 26.5 GHz. Third, reproducibility of the microwave data has been verified for three CPW devices, using several successive fluidic assemblies on each. Only the interference structure changes slightly from device to device.

The most striking aspect of the microwave data is that the transmission through the hemoglobin and bacteria specimens is higher than that through their respective buffer samples. In addition, the response due to 100  $\mu\text{g/mL}$  of hemoglobin is far stronger than that for DNA, even though the DNA is more concentrated (500  $\mu\text{g/mL}$ ). Furthermore, the hemoglobin exhibits increased transmission across a frequency range from <100 MHz to 25 GHz, which is unique among the samples measured to date (by contrast, the onset of increased transmission in the bacteria data is at  $\approx 1$  GHz). The increases in transmission are not correlated with any change in reflection, indicating that there is a decrease in power dissipation within the sample. Finally, the breadth of the response implies that there is no resonant process at play (as is also the case for the *E. coli* data). We must therefore conclude that the increased transmission represents an increase in the transparency of the medium to microwaves, i.e., that these specimens are "better" dielectrics than water alone at this frequency. The fact that this frequency range coincides with the  $\gamma$ -dispersion transition in water (implying high dissipation) is most likely a contributing factor to the success of detection.

Other samples measured, for which data are not shown here, include collagen, bovine serum albumin, and ribonucleic acid solutions. These macromolecule solutions exhibit behavior highly similar to that of the DNA in Fig. 3(b) (i.e., with the 10–20 GHz interference features present) and *not* to that of the buffer solution. This raises the possibility that the strength and shape of the interference features are more sensitive to the presence of macromolecules and their counterion clouds than just to simple salts. Again, it is reasonable to conclude that this frequency range is significant due to the  $\gamma$ -dispersion of water. The reason for the strength

of transmission enhancement by hemoglobin, compared to that by nucleic acids or other proteins, is yet to be confirmed, but we hypothesize that it is associated with the activity of the central heme complex.

In summary, we have developed coplanar wave guide devices to analyze small volumes of biological samples confined within a microfluidic channel or well. These devices yield permittivity spectra across an exceptionally broad range of frequencies: from 40 Hz to 26.5 GHz thus far. Neither chemical treatment nor surface activation is required. By combining transmission line design with robust thin-film insulation, sensitivity to sample properties can be achieved in both low- and high-frequency regimes within a single device. We observe transmission enhancements, with different frequency dependences, for hemoglobin solutions and suspensions of *E. coli* bacteria.

The authors acknowledge the invaluable assistance of N. Jarosik, E. Fitzpatrick, H. Tran, L. Page, and D. T. Wilkinson, and the use of equipment from the Microwave Anisotropy Probe project. Work was funded in part by the NSF, DARPA, ARO, and the NJ Commission on Science and Technology.

- <sup>1</sup>S. Nie and R. N. Zare, *Annu. Rev. Biophys. Biomol. Struct.* **26**, 567 (1997).
- <sup>2</sup>S. Weiss, *Science* **283**, 1676 (1999).
- <sup>3</sup>G. MacBeath and S. L. Schreiber, *Science* **289**, 1760 (2000).
- <sup>4</sup>J. Viovy, *Rev. Mod. Phys.* **72**, 813 (2000).
- <sup>5</sup>L. L. Sohn, O. A. Saleh, G. R. Facer, A. J. Beavis, R. S. Allan, and D. A. Notterman, *Proc. Natl. Acad. Sci. U.S.A.* **97**, 10687 (2000).
- <sup>6</sup>H. Fricke, *Philos. Mag.* **14**, 310 (1932).
- <sup>7</sup>K. S. Cole and R. H. Cole, *J. Chem. Phys.* **9**, 341 (1941).
- <sup>8</sup>K. Asami, E. Gheorghiu, and T. Yonezawa, *Biophys. J.* **76**, 3345 (1999).
- <sup>9</sup>C. Prodan and E. Prodan, *J. Phys. D* **32**, 335 (1999).
- <sup>10</sup>G. Smith, A. P. Duffy, J. Shen, and C. J. Olliff, *J. Pharm. Sci.* **84**, 1029 (1995).
- <sup>11</sup>H. E. Ayliffe, A. B. Frazier, and R. D. Rabbitt, *IEEE J. Microelectromech. Syst.* **8**, 50 (1999).
- <sup>12</sup>J. Hefti, A. Pan, and A. Kumar, *Appl. Phys. Lett.* **75**, 1802 (1999).
- <sup>13</sup>J. M. Cooper, *Trends Biotechnol.* **17**, 226 (1999).
- <sup>14</sup>D. C. Duffy, J. C. McDonald, O. J. A. Schueller, and G. M. Whitesides, *Anal. Chem.* **70**, 4974 (1998).
- <sup>15</sup>H. P. Schwan and S. Takashima, *Encyclopedia of Applied Physics* (VCH, New York, 1993), Vol. 5, pp. 177–200.
- <sup>16</sup>P. Debye, *Polar Molecules* (Dover, New York, 1929).
- <sup>17</sup>G. De Gasperis, X. Wang, J. Yang, F. F. Becker, and P. R. C. Gascoyne, *Meas. Sci. Technol.* **9**, 518 (1998).
- <sup>18</sup>A. K. Jonscher, *Nature (London)* **267**, 673 (1977).
- <sup>19</sup>B. Onaral, H. H. Sun, and H. P. Schwan, *IEEE Trans. Biomed. Eng.* **31**, 827 (1984).
- <sup>20</sup>P. A. Cirkel, J. P. M. van der Ploeg, and G. J. M. Koper, *Physica A* **235**, 269 (1997).
- <sup>21</sup>J. Gimsa and D. Wachner, *Biophys. J.* **75**, 1107 (1998).
- <sup>22</sup>V. Raicu, *Phys. Rev. E* **60**, 4677 (1999).

Applied Physics Letters is copyrighted by AIP Publishing LLC (AIP). Reuse of AIP content is subject to the terms at: <http://scitation.aip.org/termsconditions>. For more information, see <http://publishing.aip.org/authors/rights-and-permissions>.